EAI Endorsed Transactions
on Scalable Information Systems
Research Article **EAI.EU**

Optimization of Larch Timbering Cross Section Based on Finite Element

Wei Wang*

College of Mechanical and Electrical Engineering, Northeast Forestry University, Harbin, 150040, China.

Abstract

In view of the problem of the low utilization rate of larch as building materials, the cross-sectional dimension of larch wooden beams was optimized in this paper. The size of the larch wooden beam is 2000mm×80mm×80mm and the moisture content is 8.45%. By measuring experiments, The larch was statically analyzed by finite element softwareWith the volume of the beam as the target function, cross-section height and width as design variables, maximum stress and maximum deformation as state variables, and the results of static analysis as the state variable. Using these dates as the constraint of optimization design, the cross-sectional dimension of the larch wooden beam has been optimized as 2000 mm long, 55.02mm wide and 110.3mm high. The material was saved approximately 5.5% compared with that before optimization and improved the utilization efficiency of larch wooden beams in the construction industry.

Keywords: larch, availability, finite element, optimization.

Received on 11 January 2022, accepted on 20 January 2022, published on 26 January 2022

doi: 10.4108/eai.26-1-2022.172998

1. Introduction

The latch is one of the major species of alpine coniferous forests in northeast, north and southwestern China. [3] is widely used in civil and public buildings in Europe, North America, Japan, and other regions due to its fast growth rate, decay resistance, low density, high strength, excellent seismic performance, and a positive impact on the indoor environment. However, larch wood also has many defects, such as a large shrinkage coefficient, easy cracking, easy severe deformation during processing, growth stress and residual drying stress during processing, and poor size stability [4-6]. Many scholars at home and abroad have conducted an extensive and in-depth study of the classification and full-size mechanical properties of [7-8], due to the lack of full-size mechanical test data of plantation larch, limited the application of plantation wood in the field of wood structure materials and wood structure construction [9]. Therefore, how to efficiently and reasonably use and improve the wood performance, and improve the utilization rate of the larch, has become the focus of the majority of forestry workers.

To construct frame structures using planted larch and grade timber by stress, substantial sample tests are dramatically required, especially those based on full-size timber to provide basic data support for necessary calculations in timber design. Size wood is processed into wood [10] of a specified size according to standards or specifications. The elastic modulus (MOE) of size wood is the key [11] for wood grading and wood structure design, especially for determining the deflection level [12-13] that meets the normal use limit state under bending conditions. The elastic modulus of sized wood is usually studied by static testing, but such testing procedures are time-consuming, labor-intensive, and may damage the wood. Lee et al. [14] used carbon fiber reinforced polymer (CFRP) to further enhance the effect of wood shear strength, reinforcing the average connection strength and yield shear strength of larch. Tumenjargal et al. [15] evaluated the larch elastic modulus (MOE) and rupture modulus (MOR) and found a relationship between MOE and MOR. Azeufack et al. [16] developed non-destructive testing (NDT) to replace static testing methods and determine the dynamic elastic modulus of wood, which is more convenient and time-saving when compared to testing methods, and most importantly, they do not damage the wood. Common non-destructive detection techniques include the transverse vibration method,

* Corresponding author. Email: 236997574@qq.com

longitudinal base frequency vibration (FFV) test method and stress wave method, which consider the mechanical properties of wood [17-18] according to different parameters. Xie [19] studied the role of connection structure on the mechanical properties and analyzed the size impact of connection components on the mechanical properties. Han et al. [20] used the reliability analysis method and obtained the design value of the ultimate compressive strength (UCS) of ordinary size Chinese larch wood. Ren et al. [21] developed a finite element model to investigate the mechanical properties under transverse compression. Xie et al. [22] explored the residual compressive strength, tensile strength, and shear strength parallel to the sample particles, using different temperatures and cooling methods. Promote the utilization of natural larch in production and processing, and determine the optimal processing time of wood, [23]. At present, many research scholars have used the finite element method to optimize [24-28] for industrial applications, control systems and machine parts, but it is rare to apply this method in the field of wood construction.

This paper uses ANSYS software to analyze the structure common in practical engineering, obtain the maximum deformation and maximum bending stress, check the safety strength, and then the section size of the cantilever was optimized by ANSYS software. The finite element software ANSYS was used to analyze the maximum deformation and maximum stress, optimize the cross-section size of larch beam as the target function, section height and width as the design variable, maximum stress and maximum deformation as the state variable, and the result of static analysis as the constraint, so the minimum volume of the beam, the most material, the lowest manufacturing cost and improve the wood utilization.

2 Data Measurement and Modeling Analysis

2.1 Material Properties Measurement

For wood materials used in construction or home decoration, the moisture content is generally about 8% after drying, which is an appropriate amount. Moisture content is too high or too low will lead to quality problems. During experimental design, the moisture content of larch wood beams after drying is 8.45%. Wood elastic constants mainly include modulus of elasticity, modulus of shearing j and Poisson's ratio. Modulus of elasticity includes the constants in three directions: the direction parallel to grain (L direction), radial (R direction) and tangential (T-direction):

$$E_i = {\sigma_i}/{c} \quad (i = L, T, R) \tag{1}$$

To find the Poisson's ratio, in the condition when only positive stress exists in the direction of *i*, and other stress is absent, the ratio between the strain of *j* direction and *i* direction is negative.

$$\mu_{ij} = -{\varepsilon_{ij}}/{\varepsilon_i} \quad (i, j = L, T, R) \tag{2}$$

GLR, GTR, GLT stand for the shear elastic modulus in the surface of LR, RT, LT respectively; 45°test specimen and the following formula is used to calculate the shear modulus:

$$G = \frac{\Delta P_{45^\circ}}{2A_0(\Delta\varepsilon_x - \Delta\varepsilon_y)} \tag{3}$$

In the formula, *G* stands for shear modulus(Mpa);

ΔP_{45° represents the initial load increment on the loading strain curve;

$\Delta\varepsilon_x$ represents the strain increment to the specimen along the axial direction of the specimen corresponding to ΔP;

$\Delta\varepsilon_y$ represents the strain increment in the direction perpendicular to an axial direction of the specimen;

A_0 indicates the cross-sectional area of the specimen (mm^2).

Data measurement results are shown in Table 1.

Table 1. 12 elastic constants of larch wood beams

E_L(Mpa)	E_R(Mpa)	E_T(Mpa)	G_{LR}(Mpa)	G_{TR}(Mpa)	G_{LT}(Mpa)	μ_{TL}	μ_{LT}	μ_{RL}	μ_{LR}	μ_{RT}	μ_{TR}
9845	845	482	633	767	232	0.33	0.023	0.41	0.028	0.52	0.75

2.2 larch wooden beams Finite Element Analysis

2.2.1 Setting of unit type of wood beams and material properties

The article needs to analyze the static performance of larch wooden beams. The unit type selected in this paper is Solid 45, this unit, possessing good plasticity, high creep resistance, expansion, large deformation, large strain, also has Stiffening anisotropy and other functions. Therefore Solid 45 is selected as the unit model for larch wooden beams and spacer model.

When defining the characteristics of the material, the material is arranged to be orthotropic. All the coefficients in this paper are defined by using the column regularization method, to archive better rationality and a high degree of consistency.

2.2.2 Analysis model of wooden beams

ANSYS software uses the dimension of 2000mm×80mm×80mm to simulate larch wooden beams. 2000mm is the *X* direction. Steel gaskets with a size of 80mm×80mm×20mm are adopted at the position of constraints and load. The role of steel gasket is to prevent stress concentration in the course of analysis. The gasket is set to be rigid gaskets with the material possessing linear and isotropic elastic.

In addition, the modulus of elasticity of the gasket should be set at infinity, to achieve the effect of preventing stress concentration. However, if the elastic modulus of the rigid gaskets outnumbers the timber specimen too much can lead to non-converging analysis results. Therefore, the elastic modulus of the gasket herein is set at 1×109MPa, Poisson's ratio is at 0.2. Larch wooden beams model is shown in Figure 1.

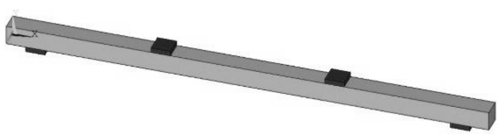

Figure 1. Larch wooden beam model

2.2.3 Meshing

After determining the type of unit and setting the material properties. Meshing the model is the next step, and meshing used in this paper is the mapping mesh with the length of 20 mm, which can control the density and quality of element mesh dividing. What important is the relatively less amount of time-consuming calculations performed within the whole process? The division of the grid is shown in Figure 2.

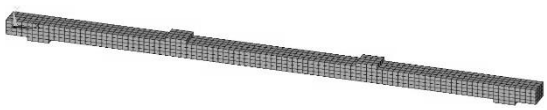

Figure 2. The meshing of larch wood beams

2.2.4 Deploying load

After complete meshing, the loading model and constraints are applied to find the solution. Load deployed is the monotonic vertical force on a central node of two gaskets in the model, the resultant force is 1000N. Constraints are arranged in displacement in the *Y* direction between the centerline position of two supporters, which allows free rotation of the gasket around the Z-axis, reducing the excess binding effect of the gasket on the specimen.

2.2.5 Analysis of the results

In this paper, the maximum stress criterion was used to solve the stress in all directions. Maximum normal stress is also known as "the maximum tensile stress." Under the condition of complex stress, the composite will be in a failure state if one or several stresses are equal to its strength limit. In other words, the stress within material should be smaller than the stress of one or several main directions. Otherwise, the material will be damaged. The discriminant formula of maximum normal stress theory is given by: for tensile stress,

$$\sigma_1 < X_T \quad \sigma_2 < Y_T \quad |\tau_{12}| < S \tag{4}$$

For compressive stress:

$$\sigma_1 > -X_C \quad \sigma_2 > -Y_C \tag{5}$$

In the formula above, there is no relationship between the variables. If such set of inequality is not satisfied, the material will be damaged due to X_T、X_T、X_T、X_T or S failure mechanism. When applying the maximum stress theory, the stress in the material needs to be converted to the stress in the main direction of the composite. The final results of the analysis are shown in Figure 3.

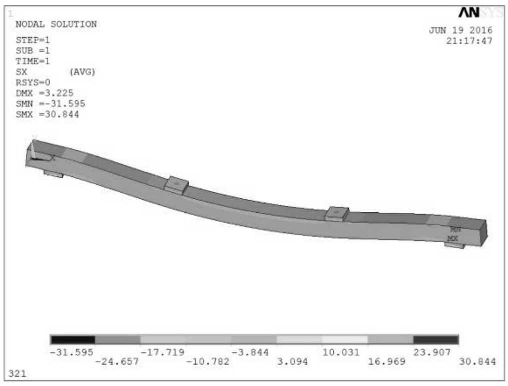

(a) X-direction stress diagram

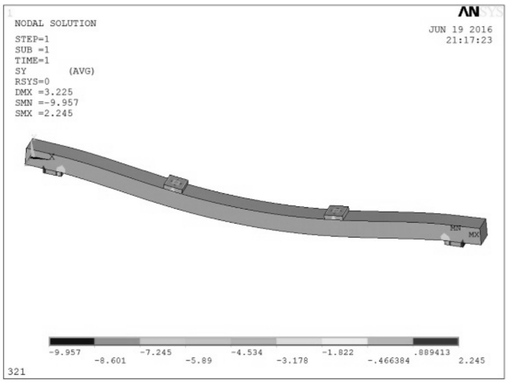

(b) Y-direction stress diagram

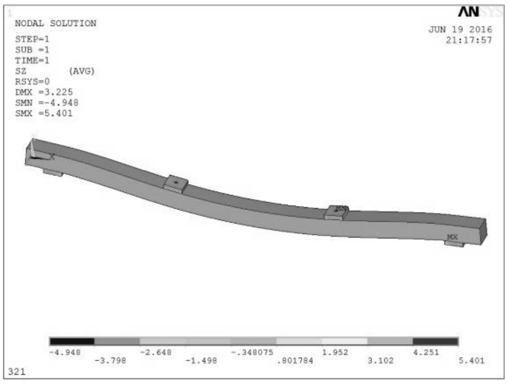

(c) Z-direction stress diagram

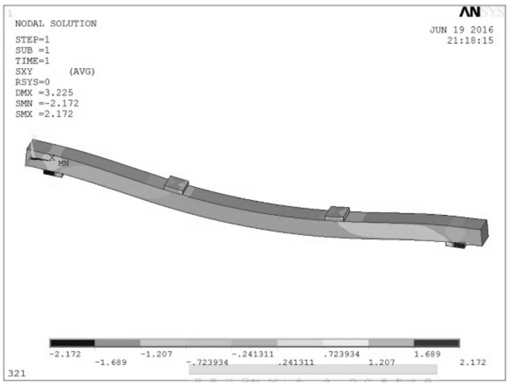

(d) XY-direction shear stress diagram

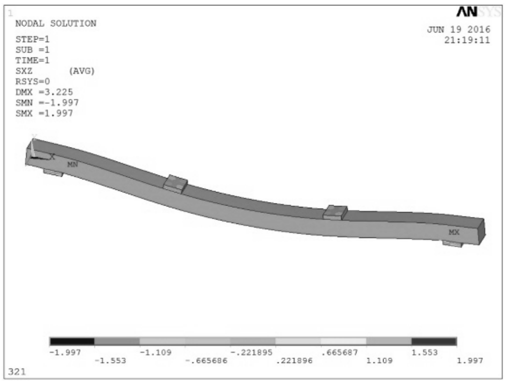

(e) XZ-direction shear stress diagram

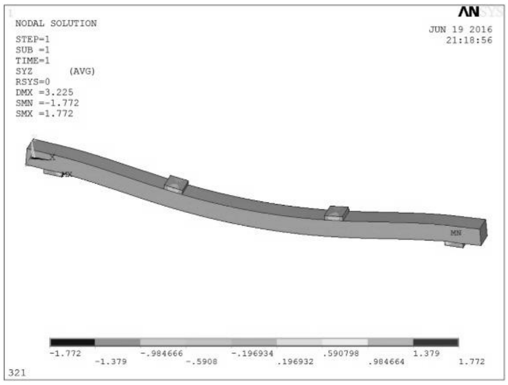

(f) YZ-direction shear stress diagram

Figure 3. Figure stress larch wood beams in different directions

According to the general HILL yield criterion, maximum equivalent stress is determined by the formula below:

$$\sigma_e = \left(\frac{1}{3} \{\sigma\}^T [M] \{\sigma\} - \frac{1}{3} \{\sigma\}^T [L] \right)^{\frac{1}{2}} \tag{6}$$

where $\{\sigma\}^T$ stands for the stress in the respective direction.

$$[L] = \{L_1 \quad L_2 \quad L_3 \quad 0 \quad 0 \quad 0\}^T$$

$$M = \begin{bmatrix} M_{11} & M_{12} & M_{12} & 0 & 0 & 0 \\ M_{21} & M_{22} & M_{23} & 0 & 0 & 0 \\ M_{31} & M_{32} & M_{33} & 0 & 0 & 0 \\ 0 & 0 & 0 & M_{44} & 0 & 0 \\ 0 & 0 & 0 & 0 & M_{55} & 0 \\ 0 & 0 & 0 & 0 & 0 & M_{66} \end{bmatrix}$$

The variation of the maximum equivalent stress according to the solution is shown in Figure 4.

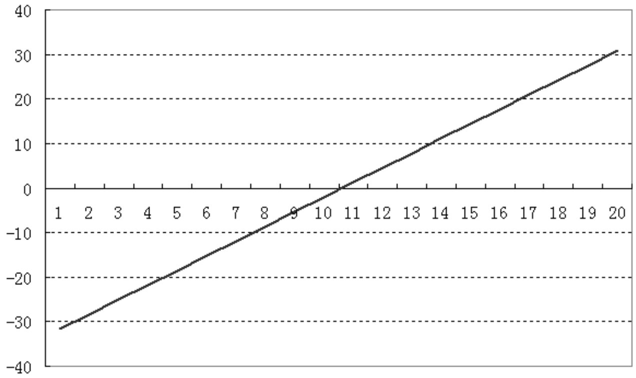

Note: The straight line is the maximum equivalent stress

Figure 4. Model equivalent maximum stress curve

Based on the changes of the value of the stress in different directions in Figure3, the maximum stress curve for the model can be drawn with ANSYS time mileage processor, which is shown in Figure4. Figure 3(a, b, c, d, e, f) can visualize the changes, maximum and minimum of the stress in all directions. The maximum equivalent stress of 30.844Mpa was obtained from the model in Figure 4, and was taken to be the optimized design constraints.

3. Optimization on the sectional dimension of larch wood beams

3.1 Basic parameters of optimization

The larch wooden beams are simplified as ANSYS program BEAM3 unit model, applying constraints located 120mm and 1880mm, deploying force at the location of 640mm and 1360mm. Parameter constraint is the maximum allowable stress value, which is determined to be 30.844mpa. According to the regulation in Beam Design Manual, the maximum deflection of the wood beam should be less than *L*/400, where *L* represents the length of the specimen. So the degree of deflection herein is 5mm. The height, width is set to be greater than or equal to 40mm. In the optimization process, the volume of wood beams is determined. According to tas the objective function, the height and width of wooden beams are design variables, maximum stress and maximum degree of deflection as state variables. The objective function value convergence tolerance is taken as 0.01, a zero-order optimization method is used here.

3.2 Optimization Mathematical Model

This design optimization model is as follows:

$$\min f(x) = \begin{cases} x = (B, H, S_{\max}, D_{\max}) \\ 10 \le B \le 40 \\ 10 \le H \le 40 \\ S_{\max} \le F_{\max} \\ D_{\max} \le 5 \end{cases} \tag{7}$$

The objective function is a function of volume (mm³).

B, H represents the width and height, the design variables (mm);

$S_{\max}$ represents the maximum stress, a state variable;

$F_{\max}$ is the maximum equivalent stress (Mpa) as solved above;

$D_{\max}$ represents the maximum degree of deflection, a state variable (mm).

3.3 Optimization Results

According to the above question, creating the specimen optimizing design model, load and constraints, then finding a solution based on the model established, and finally entering the optimization constraints for optimization analysis, larch wood beams optimization is performed following the steps above. Table 2 shows data calculated for each optimization, 20 sets of data in total, including the result of the 10th cycle as the optimal solution (in Table 2, the result marked "*" are our optimum design list). When the width (*B*) is 55.02mm, height (*H*) is 110.3mm, the state variable $S_{\max}$ = 26.34Mpa, $D_{\max}$ = 2.52mm, the total volume of the beam appears at the best value. The optimal solution for the volume of 1.21 × 107mm^3.

Sectional dimension optimized according to Table 3 is more reasonable than the original, also reducing the volume of 7.0×10^5 mm^3, saving an estimated amount of 5.5 percent of larch material.

Table 2. Optimization results on the cross-section of larch wooden beams

Optimization No.	According With judgment	B (mm)	H (mm)	S_{max} (Mpa)	D_{max} (mm)	Volume (mm^3)
1	FEASIBLE	80.00	80.00	30.84	3.23	1.28×10^7
2	FEASIBLE	70.25	121.3	28.42	0.91	1.69×10^7
3	FEASIBLE	78.42	99.42	12.32	0.65	1.54×10^7
4	FEASIBLE	63.16	97.41	25.74	1.02	1.28×10^7
5	FEASIBLE	88.11	87.25	2.78	0.43	1.53×10^7
6	INFEASIBLE	59.90	89.24	34.31	6.21	1.05×10^7
7	FEASIBLE	76.42	96.53	16.42	0.56	1.46×10^7
8	FEASIBLE	74.04	97.31	18.45	0.32	1.43×10^7
9	FEASIBLE	72.42	87.25	21.42	1.41	1.25×10^7
10	FEASIBLE	55.02	110.3	24.19	2.51	1.21×10^7
11	FEASIBLE	54.54	126.6	18.56	1.23	1.36×10^7
12	FEASIBLE	68.24	90.05	4.67	1.11	1.23×10^7
13	INFEASIBLE	75.02	100.22	35.42	2.03	1.51×10^7
14	FEASIBLE	70.31	91.65	3.19	1.05	1.26×10^7
15	FEASIBLE	70.00	95.49	17.31	1.51	1.33×10^7
16	FEASIBLE	69.69	94.89	23.12	1.12	1.31×10^7
17	FEASIBLE	68.00	94.11	28.00	1.21	1.28×10^7
18	FEASIBLE	79.12	84.65	17.31	0.55	1.34×10^7
19	INFEASIBLE	78.62	84.46	34.43	2.02	1.33×10^7
20	FEASIBLE	78.89	88.02	3.45	1.08	1.39×10^7

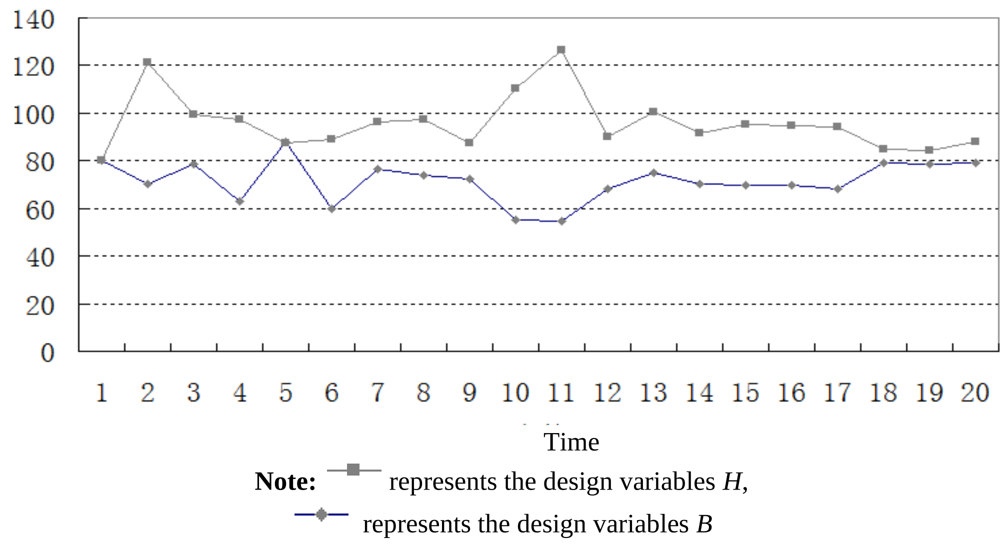

Figure 5. Curve design variables

The design variables shown in Figure 5 change to the values of *B* and *H* of the minimum volume, namely *B*=55.02mm, *H*=110.3mm.

Table 3. Optimize the larch beam section dimensions before and after

	Volume (mm^3)	*B* (mm)	*H* (mm)	Volume saving (mm^3)	Percentage saving (%)
Before optimization	1.28×10^7	80.00	80.00	7.0×10^5	5.5
After optimization	1.21×10^7	55.02	110.3		

4. Conclusion

Through experiments, ANSYS simulation and ANSYS software optimization design, the cross-sectional size of larch wood beams selected in this article has been optimized, while savings approximately 5.5% of the raw material compared with that before optimization, improving the utilization efficiency of larch wood beams in the construction industry. Meanwhile, the paper introduces the finite element method for modeling analysis of larch wood beams, which belongs to cross-disciplinary study, providing foundation and inspiration for the analysis of other composite materials. Furthermore, this article selects larch material with a moisture content of 8.45%, also lays the theoretical foundation for the analysis of other materials of larch and other types of wood with different moisture content.

References

[1] Tian Z, Wang Z, Wang J.et al. Classification in Modulus of Elasticity and Mechanical Properties of Larch Lumber in Mohe. Northwest For. Univ. 2017; 32(3): 211–215.

[2] Zhong Y, Wu G, Ren H. Design Value of Tension of Domestic Dimension Lumber for Structural Use. Scientia Silvae Sinicae. 2018; 54(4): 100–112.

[3] Švajlenka, Jozef, M Kozlovská. Houses Based on Wood as an Ecological and Sustainable Housing Alternative—Case Study. Sustainability. 2018; 10(5): 1502-1521.

[4] Zhaopeng T, Junhua X, Mingyue L. Characteristic Value of the Modulus of Elasticity (MOE) for Natural and Planted Larch in Northeast China. Forests. 2021; 12(7): 883-895.

[5] Brol J, Wdowiak-Postulak A. Old Timber Reinforcement with FRPs. Materials. 2019; 12(24): 4197-4209.

[6] Peng Wei, Pukkala. et al. Optimal management of larch (Larix olgensis A. Henry) plantations in Northeast China when timber production and carbon stock are considered. ANNALS OF FOREST SCIENCE. 2018; 75(6): 63-77.

[7] Xianliang Zhang, Xue Li, Rubén D Manzanedo, et al. High risk of growth cessation of planted larch under extreme drought. IOP Publishing. 2021; 16(1): 1-10.

[8] Minjuan He, Xiaofeng Sun, Haiqing Ren, et al. Experimental study on the system effect of bending cross-laminated timber fabricated with Karamatsu larch. Construction and Building Materials, 2021; 299(7):1-9.

[9] Ji Y, Xu P, Chen J Y. An hourly electricity consumption calculation method for hvac terminal units with classification and regression tree on the basis of sub-metering. IOP Conference Series Earth and Environmental Science. 2019; 238(1): 1-7.

[10] Hu S, Peenko R, Hozjan T. Predicting the thickness of zero-strength layer in timber beam exposed to parametric fires. Engineering Structures. 2021; 229(2021): 1-11.

[11] Wang H. An Investigation of the Duration of Load of Structural Timber and the Clear Wood. Forests. 2021; 12(9): 1148.

[12] Zhu Y. J Yao. A Novel Reliability Assessment Method Based on Virtual Sample Generation and Failure Physical Model. 2018 12th International Conference on Reliability, Maintainability and Safety (ICRMS); 2018.10.01; Shanghai; 2018.

[13] Y J Song, S I Hong. Compressive Strength Properties Perpendicular to the Grain of Larch Cross-laminated Timber. Bioresources. 2019; 14(2): 4304-4315.

[14] In Hwan Lee, Y J Song, S I Hong. Tensile Shear Strength of Steel Plate-reinforced Larch Timber as Affected by Further Reinforcement of the Wood with Carbon Fiber Reinforced Polymer (CFRP). Bioresources. 2021; 16(3): 5106-5117.

[15] Tumenjargal B, Ishiguri F, Takahashi Y, et al. Bending properties of dimension lumber produced from Siberian larch (Larix sibirica) in Mongolia. Journal of Wood Science. 2020; 66(1): 17-24.

[16] Azeufack U G, Kenmeugne B, Foadieng E, et al. Mechanical Characterization and Measurement of the Damage of Pericopsis elata (Assamela). World Journal of Engineering and Technology. 2019; 07(2): 256-269.

[17] Castro D, Matvieieva N, Grosso M, et al. Evaluation of Mode II Delamination Area by Non-destructive Techniques: Accuracy and Influence on Fracture Toughness Calculation. Journal of Nondestructive Evaluation. 2021; 40(3): 58-68.

[18] Pranata Y A, Kristianto A, Darmawan A. Elastic Cross-Section Modulus Ratio of Jabon (Anthocephalus cadamba Miq.) Bolt-Laminated Timber Beams. IOP Conference Series Materials Science and Engineering. 2021; 1071(1): 1-16.

[19] Xie X. Experimental and Analytical Analysis of Mechanical Properties for Large-Size Lattice Truss Panel Structure Including Role of Connected Structure. Materials. 2021; 14 (17): 5099.

[20] Han L, X Zhao, Zhou H, et al. Reliability Analysis on Compression Strength Property of Chinese Larch Visually-Graded Dimension Lumber. Wood Research. 2019; 63(3): 471-482.

[21] Ren H. Study of the Mechanical Properties of Wood under Transverse Compression Using Monto Carlo Simulation-Based Stochastic FE Analysis. Forests. 2022; 13(1): 32.

[22] Xie Q, Zhang L, Yang Z, et al. Behavior of Chinese Dahurian Larch Wood after High-Temperature Exposure: Degradation of Mechanical Properties and Damage Constitutive Model. Advances in Materials Science and Engineering. 2018; 2018(1): 1-10.

[23] Kang C W, Li C, Sun Y X. Determination of high-temperature and low-humidity treatment time for larch boxed-heart timber. Journal of Wood Science. 2020, 66(1): 22-25.

[24] Vlase S, Marin M, Öchsner, A, et al. Motion equation for a flexible one-dimensional element used in the dynamical analysis of a multibody system. Continuum Mechanics & Thermodynamics. 2019; 31(4): 715-724.

[25] Laghari R A, Li J, Laghari A A, et al. A Review on Application of Soft Computing Techniques in Machining of

Particle Reinforcement Metal Matrix Composites. Archives of Computational Methods in Engineering. 2019; 27(5): 1-15.

[26] Asif Ali Laghari, Hui He, Asiya Khan, et al. Cache Performance Optimization of QoC Framework. EAI Endorsed Transactions on Scalable Information Systems. 2019; 6(20): 1-11.

[27] Andre M Alzamora, Helder de Paula. A New Industrial Cable System Parameter Calculation Methodology Based on 3-D Finite Element Analysis. 2020 IEEE Industry Applications Society Annual Meeting; 2020.10.10; Detroit; 2020.

[28] Vlase S, Marin M, Chsner A. Gibbs–Appell method-based governing equations for one-dimensional finite elements used in flexible multibody systems. Continuum Mechanics and Thermodynamics. 2020; 33(6): 357-368.